JOURNAL OF OPTOELECTRONICS AND ADVANCED MATERIALS, Vol. 11, No. 5, May 2009, p. 625 - 634

Phase separation due to high temperature annealing of sputtered SiO_x layers

N. KARPOV[a], V. VOLODIN[b,a], J. JEDRZEJEWSKI[c], E. SAVIR[c], I. BALBERG[c], Y. GOLDSTEIN[c*], T.EGEWSKAYA[b], N. SHWARTZ[b], Z. YANOVITSKAYA[b]
[a]*Novosibirsk State University, 630090, Novosibirsk, Russia*
[b]*Institute of Semiconductor Physics of SB RAS, av. Lavrenteva 13, 630090, Novosibirsk, Russia*
[c]*Racah Institute of Physics, The Hebrew University, Jerusalem 91904 Israel*

SiO_x layers with lateral composition gradient (co-layers), formed by co-sputtering in argon plasma from Si and SiO_2 targets, were investigated both before and after high temperature annealing using IR absorption and Raman scattering. For all coordinates we found more oxygen in the co-layers than the oxygen amount in SiO_2 layers sputtered from quartz target only. It was found that the quartz target surface in the plasma heats up and this may result in oxygen and silicon monoxide fluxes. The capture of this additional oxygen by the silicon flux during co-sputtering may be the reason for the excess oxygen in the co-layers. For samples with low silicon content (x>1), upon annealing a complete phase separation of SiO_x into SiO_2 and Si takes place. In SiO_x films with high Si content some of the silicon is in the crystalline phase even before annealing.

(Received February 10, 2009; accepted May 25, 2009)

Keywords: Si-SiO_x system, Sputtering, Si nanoparticles, Infrared spectroscopy

1. Introduction

SiO_2 layers enriched with excess Si exhibit visible photoluminescence (PL) after high temperature annealing (HTA) due to Si nano-clusters creation. Because of this, there is quite an interest in the investigations of the properties of these layers. There is a controversy in the literature [1-3] about the precise excess Si content where maximal PL takes place. The PL spectra dependences on excess Si volume content were measured in [4,5]; the Si volume content was calculated from the thickness ratio of the one-component, Si and SiO_2 layers before annealing. This procedure is well accepted and widely used to determine the Si content in co-sputtered films. There is, however, some evidence that the Si content may change somewhat during the two-component Si plus SiO_2 sputtering.

The purpose of the present work is the investigation of the lateral distribution of Si in Si-rich SiO_2 layers (SiO_x, 0>x>2) prepared by co-sputtering from two separate Si and SiO_2 targets. The deposited layers properties are influenced by the details of the sputtering process and the experimental arrangement. The SiO_x layer made by simultaneous sputtering from two targets (named co-layer) has a lateral composition distribution of 0>x>2. From ellipsometrical data we found previously that there is excess oxygen in the co-layer in comparison to the sum of the thicknesses of the one-component layers [6]. In the present work the lateral coordinate dependences of IR transmission of SiO_2, Si and SiO_x layers before and after HTA were used for composition analyses and to clarify the process of phase separation in co-layers.

2. Background

Infra-red (IR) measurements are routinely used for determination of SiO_x layers composition [7,8]. Because most of our conclusions are based on IR transmission measurements, we are going to summarize below in some detail the known facts about IR transmission in SiO_x films. IR transmission measurements of the Si-O-Si bond vibrations were published in many papers [9-11]. Here we will consider only transverse-optical (TO) modes that were observed with a normal incidence light beam. In the wave number region of 700-1400 cm^{-1}, there are three IR absorption peaks. For instance in a typical absorption spectrum of SiO_2 obtained from a 100 nm-thick oxide film grown thermally at 1000°C on (100) silicon [9] there were observed the following peaks: 1) a peak centered at ≈810 cm^{-1} that is due to the symmetrical stretching (SS) of the O atom along a line bisecting the axis formed by two Si atoms, 2) a main peak at ≈1076 cm^{-1} and, 3) its high frequency shoulder at ≈1200 cm^{-1}. These last two are due to an asymmetrical stretch (AS) motion in which an O atom moves back and forth along a line parallel to the axis through two Si atoms. The AS motion actually gives rise to two modes, an AS_1 mode in which adjacent O atoms execute the AS motion in phase with each other, and an AS_2 mode in which adjacent O atoms execute the AS motion 180° out of phase with each other. There is no other absorption in the region between the SS and AS peaks. As is well known SiO_2 layers thermally grown on heated Si substrates have perfect quality close to fused silica [9].

In [10] IR absorption was investigated for SiO_2 layers obtained by different methods. IR absorption spectra for a pyrolytic SiO_2 layer formed at 675°C and a reactively sputtered SiO_2 layer after annealing demonstrate the same IR spectra as for SiO_2 thermo-grown layers on Si(100) substrate. On the other hand, the straight thermal evaporation of SiO_2 on unheated substrates results in SiO film formation. These SiO films show only one broad peak at 1000 cm^{-1}. This IR spectrum is quite different from that obtained for SiO_2 thermo grown layers.

As to SiO_x layers there are a few experimental articles demonstrating a linear dependence of the main peak position on x in SiO_x before annealing. The main peak position changes from 930 cm^{-1} to 1076 cm^{-1} with *x* from near 0 to 2 [11-13]. Absorption at 1076 cm^{-1} is typical for a thermal grown SiO_2 layer and it decreases with extra Si in Si rich SiO_2 layers. After annealing such a layer, the main peak position was found to shift to the position corresponding to SiO_2, suggesting a phase separation of the SiO_2 and Si phases [8]. In crystalline silicon (c-Si), vibrations due to interstitial oxygen atoms have a main IR absorption peak at 1107 cm^{-1} [14].

Performing *ab initio* calculations [15], a distinct correlation was found between Si-O bond length and the principal peak position. On the other hand, no clear correlation was found between the Si-O-Si angle and the principal peak position. Since partially oxidized Si atoms give longer Si-O bond length the above correlation suggests that the observed red shifts of the principal IR absorption peak are due to the lengthening of Si-O bonds in the suboxides. No red shift was found due to roughness of the Si/SiO_2 interface or the SiO_2 surface (only the shift due to excess Si) [16].

3. Experimental details

SiO_x films were prepared by radio frequency magnetron sputtering in an argon atmosphere. Before sputtering, the vacuum system was pumped down to a pressure of 10^{-6} Torr, then the chamber was filled with argon to a pressure of 8 10^{-3} –$1{\cdot}10^{-2}$ Torr. The power applied to each target was 60 W and the bias voltage developed on each target was -300 ± 20 V. The substrate was not intentionally heated. The sputtering configuration is shown in Fig.1. The sputtering was performed from two separated (Si and SiO_2) 2-inch targets onto a Si(001) substrate. The distance between the targets' centers was 96 mm and the distance between the targets and the substrate plane was 61 mm. The substrate was about 14 cm long and 1 cm wide and was positioned parallel to the line connecting the targets' centers. By sputtering from both targets simultaneously a continuous change of x along the SiO_x co-layer was obtained. Si layers were deposited by sputtering the Si target only, and SiO_2 layers using the quartz target only. The layers were annealed at 1100-1200 °C for 40-50 min in nitrogen flow at atmospheric pressure.

The lateral coordinate dependences along the films of the optical properties and the composition of the SiO_x layers were investigated using IR absorption and Raman scattering. To determine the IR transmission spectra of the SiO_x layers we measured the TO modes at normal incidence using a Fourier spectrometer (Infralum FT-801, "LUMEX-SIBERIA" Ltd. R&D and Production Company), designed for the spectral region of 500 – 8000 cm^{-1} with a resolution of 1 cm^{-1} and a light beam diameter of 1 mm. All Raman spectra were excited with the 514.5 nm Ar^+ laser line in the quasi-back-scattering geometry and were measured at room temperature using a double spectrometer (DFS-52, LOMO) and a cooled photo-multiplier with a spectral resolution of about 0.5 cm^{-1}.

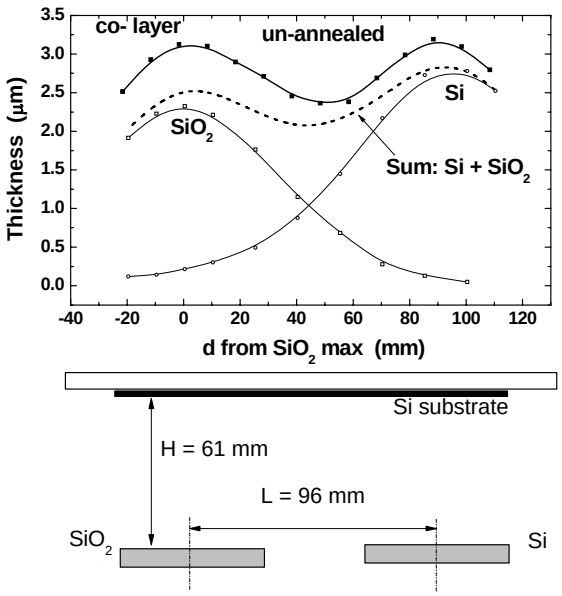

Fig.1.The sputtering configuration and the measured thicknesses of a Si layer, a SiO_2 layer, and a co-layer as functions of the lateral coordinate d. The dashed line is the calculated sum of the thicknesses of the Si and SiO_2 layers.

Fig. 1 demonstrates the sputtering configuration and the thickness dependences along the substrate of a Si film, SiO_2 film and a co-layer. The thickness was measured by a Dektak 3030 profilometer. The position of the maximum thickness of SiO_2 was chosen as the zero of the lateral coordinate d. The calculated sum of the thicknesses is shown by the dashed line, while the solid line shows the measured thickness. One can see that the measured thickness of the co-layer exceeds the sum of the thicknesses of the Si and SiO_2 layers at all coordinates. We replaced the quartz target by a silicon one to clear up the reason for this discrepancy. With the two silicon targets the thickness difference between the co-layer and two serial deposited layers remained. So the reason of the discrepancy is probably the variation of the sputtering efficiency when sputtering simultaneously from both targets.

4. Results and discussion

First the properties of the sputtered SiO_2 layers before and after annealing were investigated, in order to determine the quality of the SiO_2 layers obtained by sputtering from the SiO_2 target.

4.1. SiO_2 layers before annealing

Only one sputtering target (quartz) was used to deposit this layer; the deposition time was 35 min. The coordinate dependences of the thickness and the index of refraction of the layers were determined by ellipsometry in our previous work [6]. The maximal thickness of the layer was 590 nm (opposite quartz target, d=0) and the minimal was 20 nm (at d=100 nm). The growth rate decreases with increasing d because of the sputtering configuration (Fig.1). A change in the interference colors due to thickness variation was observed along the sample. The measured refraction index n=1.475, was coordinate independent, thus enabling us to estimate the layer thickness from the interference colors [6].

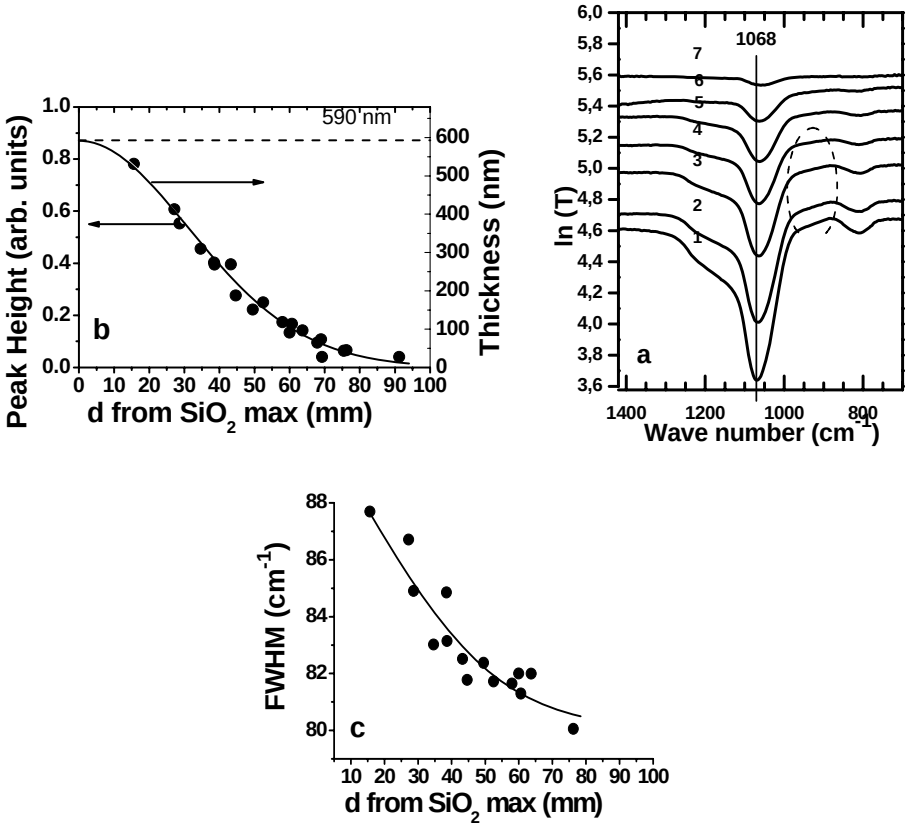

Fig.2. IR transmission spectra of a SiO_2 layer before annealing: (a) spectra at different substrate coordinates on logarithmic scale: d = 16 mm (1), 27 mm (2), 35 mm (3), 43 mm (4), 53 mm (5), 64 mm (6), 69 mm (7) mm (for clarity, the different spectra are shifted along the vertical axis). The vertical line corresponds to the minimum of curve 1. Dashed line indicates area of SiO absorption; (b) the coordinate dependence of the layer thickness – solid line and of the main peak height – symbols; and (c) the coordinate dependence of the FWHM of the main peaks.

In Fig. 2(a-c) IR transmission spectra for different samples as a function of wave number and the d coordinate dependences of the film thickness and of the main transmission peak characteristics are presented. The height and FWHM (full width at half maximum) of the peaks were obtained after IR spectra analyses using Peak Fitting Module included in OriginLab Origin 7.5. The number of peaks and their possible position were input parameters. Four peaks were used for analyses of the IR spectra in Fig. 2a.

Comparison of the peak positions (curves 1-7) in Fig. 2a with thermal SiO_2 layers shows that the main peaks are shifted to slightly lower frequencies than that obtained for thermal SiO_2 layers (1076 cm^{-1}) [9]. This shift to 1068 cm^{-1} at 590 nm (curve 1) to 1057 cm^{-1} at 20 nm (curve 7), is beyond experimental error. The red shift may be associated with elongation of the Si-O bond [15] due to sponginess and/or the presence of excess Si [16]. The narrowing of the peak from 88 to 80 cm^{-1} with decreasing thickness (Fig. 2c) is evidence of higher layer quality at lower thicknesses (lower porosity and less defects). One also expects a decrease of the refraction index because of the sponginess of the as-deposited layers, however in our SiO_2 layers at all coordinates n=1.475 that is higher than n

=1.46 for the high quality thermo grown SiO_2. In addition to the peaks corresponding to bond vibrations in SiO_2 there is also an absorption in the 900-1000 cm^{-1} range (marked with a dashed line in Fig. 2a) pointing to the presence of SiO in the layer [10]. This additional SiO can originate from the SiO_2 target that heats up during sputtering; the quartz target surface looks like fused after sputtering. It is known that during quartz evaporation a SiO layer is formed [10]. So the additional absorption in the 900-1000 cm^{-1} range, the red shift of the main peak and the higher refraction index may all be associated with the presence of SiO in the SiO_2 layer.

The main peak height of the transmission spectra is proportional to the layer thickness (Fig. 2b). So, one can estimate the oxygen amount in the layer measuring the peak height in un-annealed layers.

4.2. SiO_2 layers after annealing

IR transmission spectra of a SiO_2 layer after HTA are shown in Fig. 3a-c. The annealing was done several months after the deposition of the layer. After HTA the main peaks shift to higher frequencies (Fig.3a) and become narrower, 80-70 cm^{-1} (Fig.3c.) Simultaneously, the absorption in the 900-1000 cm^{-1} region disappears. We take this as evidence of improvement of the dioxide structure by the Si-O bond length shortening and that a separation of excess SiO into Si and SiO_2 is taking place.

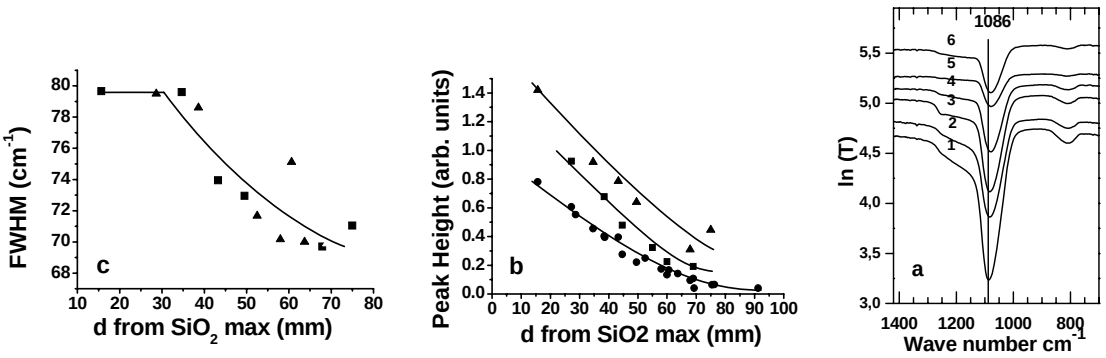

Fig.3. IR transmission spectra of an annealed SiO_2 layer: (a) spectra at different substrate coordinates: d= 16 mm (1), 35 mm (2), 43 mm (3), 50 mm (4), 68 mm (5), 75 mm (6) (the spectra are shifted along the vertical axis). The vertical line corresponds to the minimum of curve 1; (b) The coordinate dependence of the main peak height, the circles represent data before annealing; (c) the coordinate dependence of the FWHM of the main peaks. In (b) and (c), the squares and triangles represent data for annealing temperatures of 1100°C and 1200°C, respectively.

In addition, after HTA the layer thickness decreases everywhere along the sample, as evidenced by the variation of interference colors. For example, the layer thickness in the middle of the sample, 200 nm before annealing, decreased by 30-60 nm after annealing. This thickness decrease is due to layer densification [17] and of SiO evaporation from the surface layer, caused by the high annealing temperatures. As shown in Fig. 3b, despite the thickness decrease after HTA, the absorption peak heights increase. These peak increases and the decrease of FWHM can be explained by the higher quality of the SiO_2 layer after annealing. It is worth noting that after annealing the proportionality between the value of the main peak and the layer thickness disappears since now the peak value is determined substantially by the dioxide quality which in turn depends on the annealing regime.

The results presented in Figs. 2 and 3 demonstrate that the SiO_2 layers prepared by sputtering approach thermal silicon dioxide quality only after annealing.

4.3. SiO_x co-layer before annealing

The layer was deposited by co-sputtering for 30 min, its maximal thickness was 490 nm. In Fig. 4a we show the IR transmission spectra of the SiO_x layers for several lateral positions. In addition to the main absorption peak, all the spectra show an absorption region at 900-1000 cm^{-1} (marked with a dashed line) similar to the SiO_2 layers (Fig. 2a). This SiO absorption is larger than the contribution due to SiO formation from the melted quartz target observed in Fig. 2a.

Up to about the middle of the sample (d ≈ 43 mm), curves 1-4 in Fig.4a, are quite similar to those for the SiO_2 layers (Fig.2a). The peak positions for the first 4 curves in Fig. 4a are in the spectral region of 1068-1047 cm^{-1} even though for curve 4 the composition must be close to 50% of Si and 50% of SiO_2. For this composition one should expect the peak to be at about 1000 cm^{-1} [10]. A considerable peak shift and shape change of the IR spectra one can see only closer to the Si edge. There is a small peak at 1107 cm^{-1} in the curves 5-7. This frequency is typical for interstitial oxygen in the crystalline silicon phase [14]. In curves 6-7 there is no longer a peak typical for oxygen (similar to O in SiO_2) only a peak very similar to a SiO peak. The broad absorption peak for curve 7 has a maximum at 943 cm^{-1}. We notice, however, that the main peak height in all curves in Fig.4a for un-annealed SiO_x is

higher than that in Fig. 2a for unannealed SiO_2 as if there is more oxygen in SiO_x than in the SiO_2 layer.

4.4. SiO_x co-layer after annealing

The annealing in N_2 at 1200°C for 50 min was done several months after the layer deposition. The IR transmission spectra of the annealed SiO_x layer are shown in Fig. 4b for the same positions as in Fig. 4a. We see that for curves 2-7 the absorption in the spectral region 900-1000 cm^{-1} does not disappear after HTA, contrary to the SiO_2 only layers (Fig. 3a). Only for curve 1 (measured at the max of SiO_2) we observe the disappearance of this absorption.

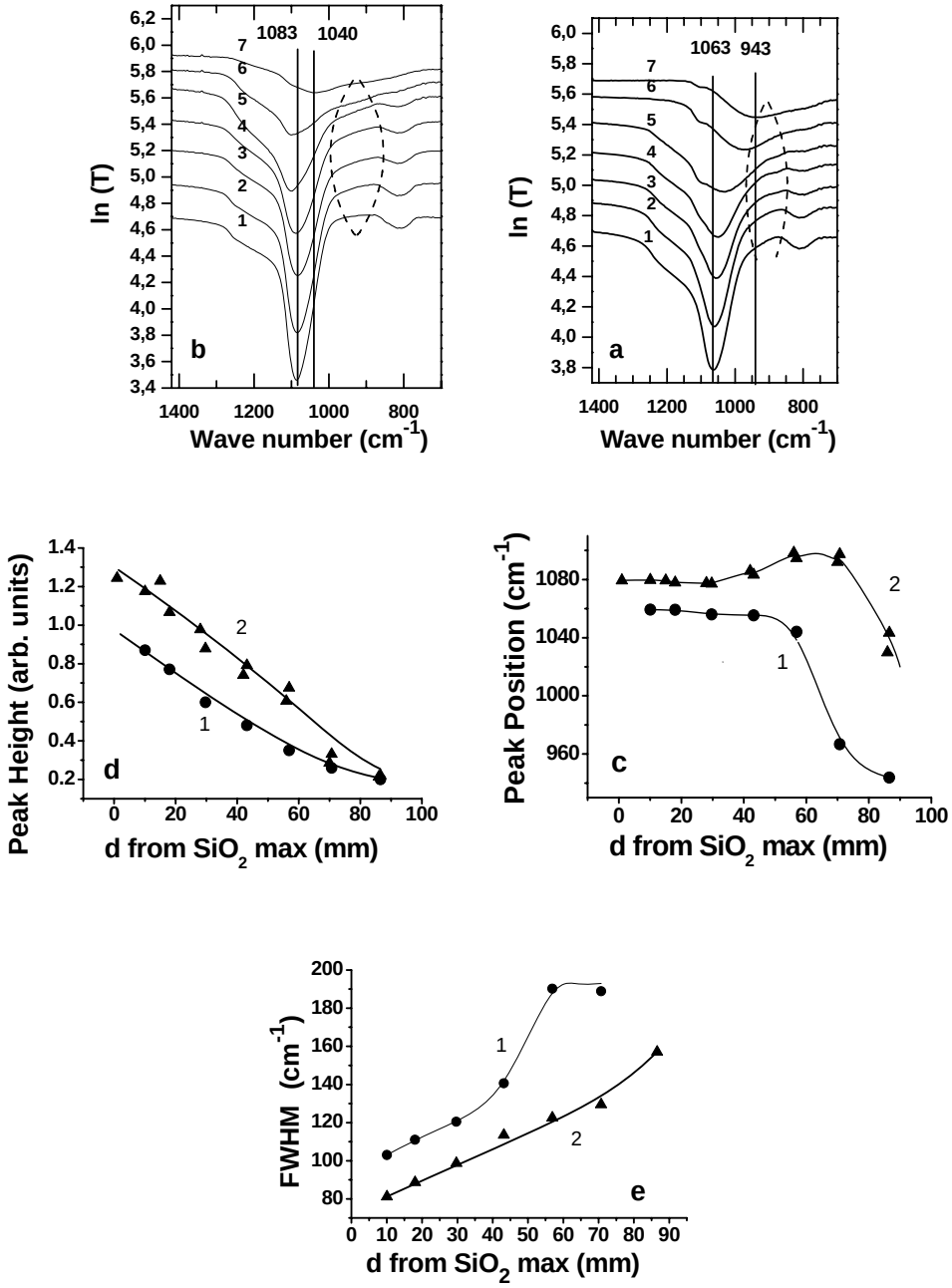

Fig.4. IR transmission spectra (T) of SiO_x layers before (a) and after (b) annealing at 1200°C in N_2 for 50 min: d = 10 mm (1), 18 mm (2), 30 mm (3), 43 mm (4), 57 mm (5), 71 mm (6), 87 mm (7) (the spectra are shifted along the vertical axis). The vertical lines in (a) and (b) correspond to peak positions of the minima in curves 1 and curves 7. Dashed line indicates area of SiO absorption. The coordinate dependences of the main peak position, peak height, and FWMH are shown in (c), (d) and (e), respectively. The circles in (e) (curve 1) represent data before annealing, the triangles (curve 2) after annealing.

The main peak positions in the first 4 curves in Fig. 4b moved to the value of thermal grown SiO_2 layer – 1083 cm^{-1}, and the peak position does not shift with increasing Si content. This points to phase separation of the SiO_x layer at low Si excess into SiO_2 and Si, like in [11]. At larger Si excess the peaks are wider (Fig. 4b, curves 5-7). There is also a tendency for the peak to shift to higher frequencies than 1083 cm^{-1} (see Fig. 4c) that may be related to the interstitial oxygen in the crystalline Si phase [14]. So we can assume that suboxide phases and interstitial oxygen are present in the film at high Si excess. A complete phase separation of the SiO_x layer doesn't take place for the samples with high Si content ($x<1$) at the given annealing conditions. The process of phase separation is nearly finished only for lower Si excess.

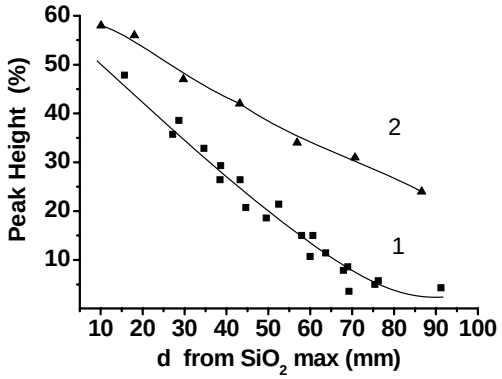

Fig.5. The coordinate dependence of the IR transmission peak heights of a SiO_2 (curve 1) and a SiO_x (curve 2) layer deposited for the same time.

The thickness of the SiO_x layers decreases after HTA according to the interference color change. At the SiO_2 edge the thickness deficiency is about 50±10 nm. The deficiency evidently depends on the coordinate along the sample. At the same time the main peak height increases after annealing (Fig. 4d) at all coordinates except the Si rich edge. For all values of excess Si the FWHM of the main peaks (Fig. 4e) decreases after annealing, as expected, however the values of FWHM are larger than those of SiO_2. The FWHM at the SiO_2 edge of SiO_x is equal to the FWHM in the SiO_2 layer (Fig. 3c) but increases with Si content. The peak height increase after HTA in spite of the decrease of the film thickness, points to the SiO_2 phase segregation. However, the peak widening indicates that the SiO_2 phase quality decreases with increasing excess Si.

4.5. Comparison of the oxygen amount in SiO_2 and SiO_x films

A priori, one expects the same oxygen amount at equal substrate coordinates in SiO_2 layers deposited only by SiO_2 target sputtering and in SiO_x layers deposited by co-sputtering of Si and SiO_2 targets. However, our results show differently. The comparison of the oxygen amount in SiO_2 and SiO_x layers was done for un-annealed samples where the proportionality between the IR peak value and layer thickness was observed. In Fig. 5 we plot the values of the main peak heights for a SiO_2 only layer (curve 1) and for a co-layer (curve 2). We see that the peak values for the co-layer are considerably higher than those for the SiO_2 only layer, especially at the Si edge of the co-layer. For annealed SiO_2 and SiO_x layers, on the other hand, such a straight comparison of peak values cannot be done since the peak values in this case are determined not only by layer thickness but also by the SiO_2 quality, as mentioned above.

In Fig. 6 we show the results of the IR spectra analyses, before and after annealing, of a SiO_2 and a SiO_x layer at two coordinate values: one near the Si edge (Fig. 6a) and the other in the middle of the samples (Fig. 6b). Fig. 6 (along with Fig. 5) demonstrates an appreciable excess of oxygen in the SiO_x layer at the Si edge in comparison with the SiO_2 layer. When contrasting the curves in the right and left parts of Fig. 6a it is apparent that the peak value in the SiO_x layer is higher than that in the SiO_2. This is true also for the curves taken at a lower Si content before annealing (Fig. 6b). Also, the peaks in the un-annealed curves on the right hand side (SiO_x) are at lower wave numbers. Upon annealing, all the peak heights increase and the peak widths decrease. This is much more noticeable for the SiO_2 layer.

We performed a best fit to the experimental curves in Fig. 6 by a minimal number of Gaussian curves. From this analysis we find that there are two appreciable peaks at low frequencies for un-annealed SiO_x in Fig. 6a. Even in annealed SiO_x layers (Fig. 6a and Fig. 6b) the peaks split up into SiO_2 (1200, 1076, 810 cm^{-1}) and SiO (near 1000 cm^{-1}) peaks. The SiO peak is much more pronounced for the sample with the higher Si content (Fig. 6a). Thus a complete phase separation of the SiO_x layer doesn't take place at the given annealing conditions for the samples with high Si content. Only for lower Si content is the process of phase separation nearly finished, as we have seen from curves 1-4 in Fig. 4b where the peak position coincides with the position for SiO_2.

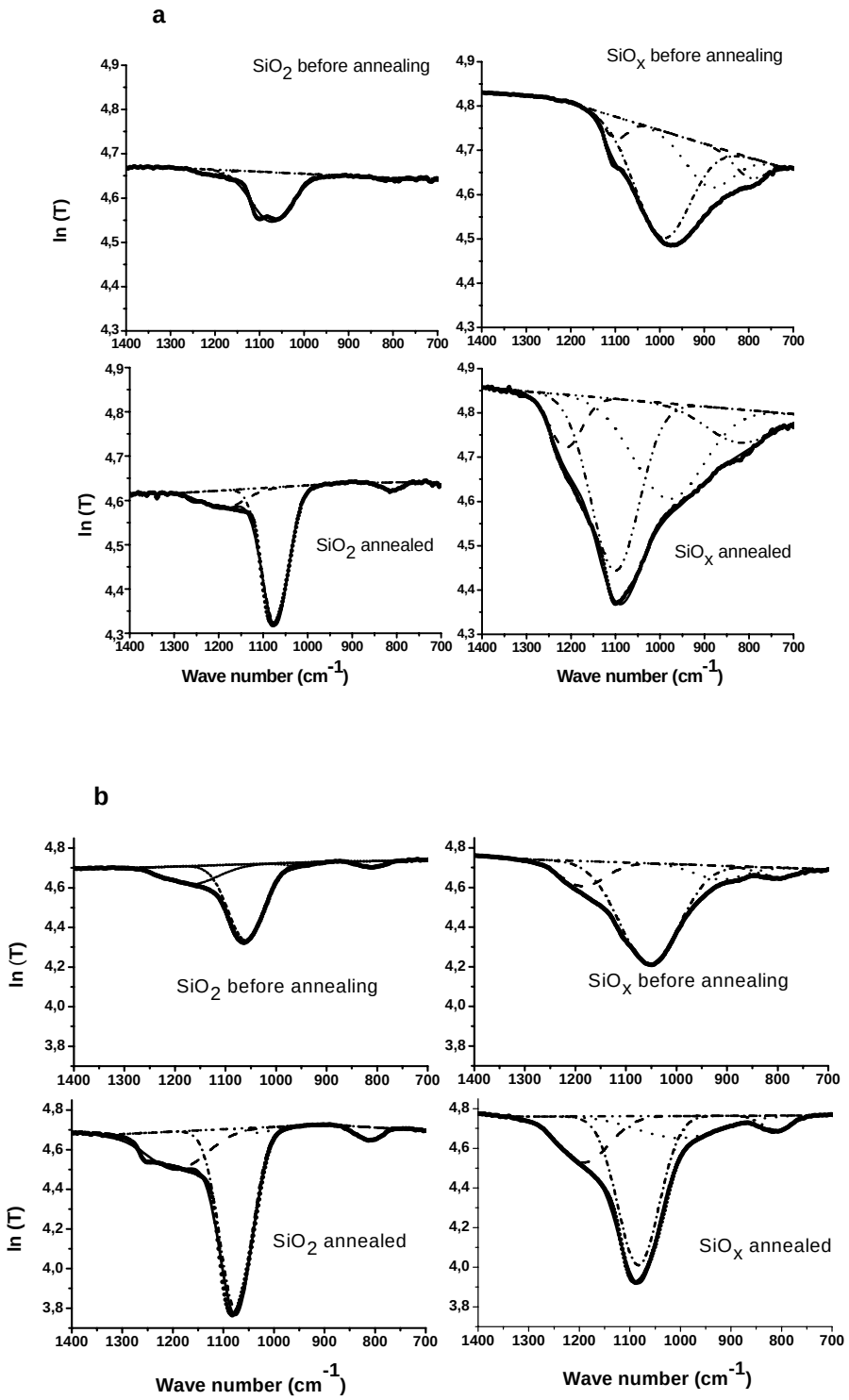

Fig.6 IR transmission spectra (T) of a SiO_2 and a SiO_x layer before and after annealing (a) d = 70 mm and (b) d = 43 mm. Solid lines – experimental IR transmission spectra, other curves - result of spectra analyses: dotted lines – SiO peak; three SiO_2 peaks: dash-dot-dot – 810 cm^{-1}, dash-dot – 1080 cm^{-1}, dash – 1200 cm^{-1}.

4.6. Source of additional oxygen

Comparison of the SiO_x spectra with those for the SiO_2 layer points to the fact that additional oxygen, over and above that coming into the SiO_2 only layer, is coming into the SiO_x layers during deposition. Now we address the source of this additional oxygen. Thick Si layers (~100 min deposition, maximal thickness 1.6) were deposited on Si substrates to check oxygen capture from the residual atmosphere in the vacuum chamber by the Si flux. The IR transmission spectra of an un-annealed Si layer are shown in Fig. 7. One can see an oxygen absorption peak for samples with different thicknesses. The absorption peaks at 867 cm^{-1} (maximal thickness, curve 1) and at 1060 cm^{-1} (minimal thickness, curve 6) are marked by arrows. Evidently, some oxygen is captured by the Si flux from the residual atmosphere during sputtering. Absence of peaks typical for SiO_2 indicates that this captured oxygen is not in the SiO_2 phase in contrast with the oxygen in co-layers (Fig. 6a, right).

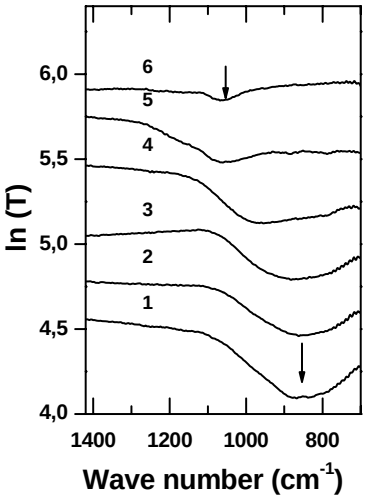

Fig.7. IR transmission spectra of a Si-layer on a Si(100) substrate before annealing at several positions with different thickness: 1-1600 nm, 2 – 1380 nm, 3 – 1100 nm, 4 – 760 nm, 5 – 550 nm, 6 – 50 nm (the spectra are shifted along the vertical axis). The peak positions at 867 cm^{-1} for maximal thickness (curve 1) and near 1060 cm^{-1} for the smallest thickness (curve 6) are shown by arrows.

To establish if additional oxygen comes to the co-layer due to co-sputtering, two types of layers were prepared. The first sample was a bi-layer, prepared by sputtering for 30 min from a SiO_2 target only and subsequently for 30 min from a Si target only, while the second layer was a co-layer co-sputtered for 30 min. Both samples were annealed for 50 min at 1200°C. In these samples the value of oxygen captured from residual atmosphere by the Si flux should be nearly the same. The transmission spectra for both these samples are shown in Fig.8. As expected, the transmission spectra in Fig. 8a for the bi-layer are similar to those shown in Fig. 3a for SiO_2 while the spectra in Fig. 8b for the co-layer are similar to those shown in Fig. 4b for SiO_x. The vertical lines in Fig. 8a and Fig. 8b correspond to peaks at 1090 cm^{-1} associated with oxygen in SiO_2 [9,10]. As above, here also in the co-layer there is clear evidence of SiO absorption at about 1000 cm^{-1} (marked by the dashed line). One can see that oxygen peaks in co-layer are larger than in bi-layer especially at high Si excess. That means that additional oxygen comes into the co-layer during the simultaneous sputtering of the SiO_2 and Si targets.

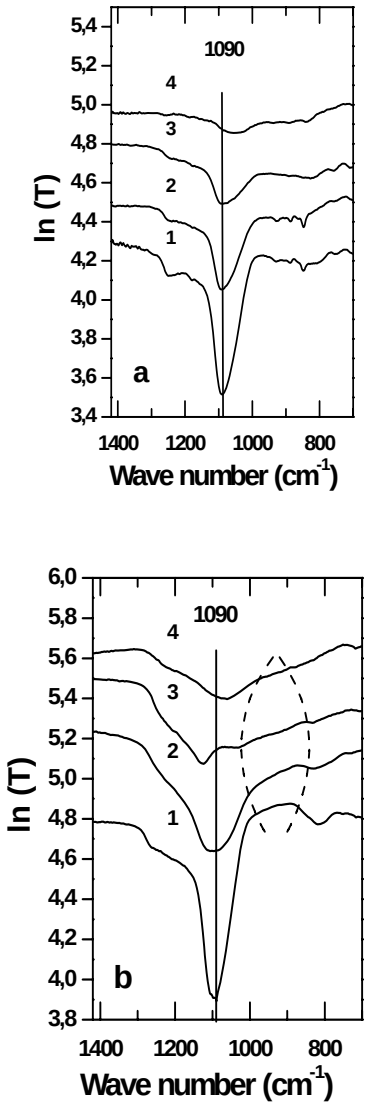

Fig.8. IR transmission spectra of annealed layers (a) - bi-layer, (b) - co-layer at coordinates d: (1) – 0 mm, (2) – 48 mm, (3) -72 mm, (4) – 96 mm. Dashed line indicates area of SiO absorption.

We assume that the quartz surface heating results not only in SiO evaporation, as was mentioned in section 3.1, but in oxygen evaporation as well. This oxygen is captured by the Si flux during co-sputtering. This would explain the presence of excess silicon at the quartz edge and excess oxygen at the silicon edge of the co-layer and thus the additional SiO absorption in the co-layer. Another assumption would be that chemical reactions in the plasma between the Si and SiO_2 fluxes take place. That would cause a redistribution of the Si and O components in the plasma and in the deposited layer.

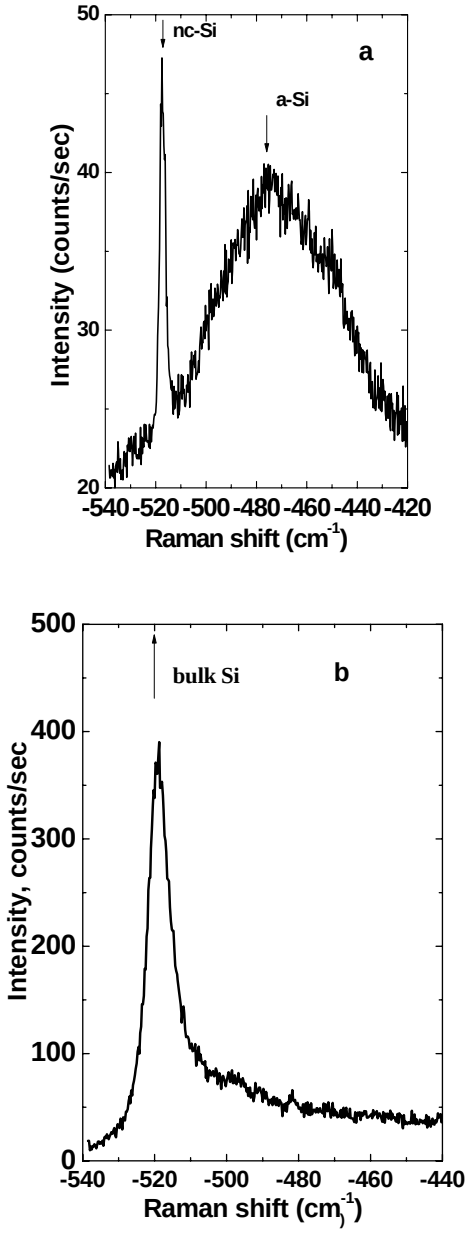

Fig.9. Raman spectra of a co-layer before (a) and after annealing (b) at coordinates d=70 mm..

It is worth noting that no additional oxygen was introduced into the layer during the annealing process. If there would be oxygen in the annealing oven, the Si rich end would be expected to be the most susceptible to oxidation during annealing. But Fig. 4b (curves 6 and 7) and the last two points in Fig. 4d demonstrate that there is no peak increase at the Si edge after annealing meaning that there is no oxygen in the annealing oven.

4.7. Raman scattering

Raman scattering measurements were carried out to check the presence of a crystalline Si phase in SiO_x layers. The expected spectrum of the nanocrystals is characterized by a narrow peak at 500-520 cm^{-1}. The spectra were measured in $Z(XX)\overline{Z}$ polarization geometry: the incident light was polarized along the $\langle 001 \rangle$ crystallographic axis and the light propagation was along the Z axis - $\langle 100 \rangle$. This geometry is forbidden for Raman scattering on longitudinal optical (LO) phonons of the Si(100) substrate, thus the chosen geometry allows us to exclude any possible Raman signal around 520 cm^{-1} from the Si substrate.

Fig. 9 shows the Raman spectra of a SiO_x layer before and after annealing. In the un-annealed sample there is a weak and broad amorphous Si peak (Fig. 9a) at approximately 480 cm^{-1} that appears as a result of the effective density of vibration modes. Thus one sees that before annealing this sample (with high excess Si content) contains mainly amorphous Si clusters except for a narrow line at 517.5 cm^{-1} indicating the presence of some Si nanocrystals (notice the enlarged scale in Fig. 9a in comparison with Fig. 9b). We estimate them to be 5-7 nm in diameter [18,19]. This peak disappears at lower excess Si content. The annealed layer shows a much larger content of nanocrystals as can be seen by the amplitudes of the peaks at about 520 cm^{-1}, see Fig. 9b. The Si clusters in the annealed samples are almost fully crystallized and their sizes increase.

5. Conclusions

The coordinate dependences of the optical properties and the composition of SiO_x co-layers, formed by co-sputtering of two separate Si and SiO_2 targets, were investigated using IR absorption and Raman scattering. For all coordinates we found more oxygen in the co-layers than the oxygen amount in SiO_2 layers sputtered from a quartz target only. This means that composition calculation by a simple addition of the thicknesses of the separately deposited silicon and quartz layers gives an understated x value in SiO_x co-layers. This excess oxygen is present only when co-sputtering from the quartz and silicon targets thus its source is not the residual atmosphere in the vacuum chamber. In SiO_x layers before annealing the amount of SiO phase increased with Si

content and remained after annealing for x<1. It was demonstrated that a complete phase separation of SiO_x into SiO_2 and Si upon annealing takes place only for low silicon content (x>1) and that in SiO_x films with high Si content, some of the silicon is in the crystalline phase even before annealing. The presence of oxygen dissolved in the crystalline silicon phase may explain the observed IR peaks in the spectral region >1100 cm^{-1} after annealing. We suggested that the fusing of the quartz target surface in the plasma may result in oxygen and silicon monoxide fluxes. The capture of this additional oxygen by the silicon flux may be the reason for the excess oxygen in the SiO_x co-layers. Another explanation could be the existence of chemical reactions between the Si and SiO_2 fluxes in the plasma. Raman scattering demonstrated that at the Si edge of the co-layer the silicon was mainly in the amorphous phase before annealing and in the crystalline phase after annealing.

Acknowledgements

This work was supported in part by the Russian Foundation for Basic Research, grant No. 06-02-72003 and in part by the Israeli Science Foundation and the Israeli Ministry of Science and Technology. I.B. holds the Enrique Berman Chair in Solar Energy Research at the HU.

References

[1] D. Comedi, O. H. Y. Zalloum, E. A. Irving, J. Wojcik, T. Roschuk, M. J. Flynn, P. Mascher, J. Appl. Phys. **99**, 023518 (2006).

[2] G.A.Kachurin, A.F.Leier, K.S.Zhuravlev, I.E.Tyschenko, A.K.Gutakovsky, V.A.Volodin, W.Skorupa , R.A.Yankov, Semiconductors. **32**, 1222 (1998).

[3] S.Guha, S.B.Qadri, R.G.Musket, M.A.Wall, T.Shimizu-Iwayama, J. Appl. Phys **88**, 3594 (2000).

[4] M. Dovrat, Y. Goshen, J. Jedrzejewski, I. Balberg, A. Sa`ar, Phys. Rev. B **69**, 155311 (2004).

[5] A. Sa'ar, Y. Reichman, M. Dovrat, D. Krapf, J. Jedrzejewski, I. Balberg, Nano Lett. **5**; 2443 (2005).

[6] A.N. Karpov, D.V. Marin, V.A. Volodin, J. Jedrzejewski, G.A.Kachurin, E. Savir, N.L.Shwartz, Z.Sh.Yanovitskaya, Y. Goldstein, I. Balberg, Semiconductors **42**, 731 (2008).

[7] R.A.B.Devine Appl. Pys. Lett. **68**, 3108 (1996).

[8] V. A. Dan'ko, I. Z. Indutnyi , I. Yu. Maidanchuk,V. I. Min'ko, A. N. Nazarov A. S. Tkachenko V. S. Lysenko and P. E. Shepelyavyi, Semiconductors, **39**, 1197, (2005).

[9] C. T. Kirk, Phys.Rev. B **38**, 1255 (1988).

[10] W. A. Pliskin, H.S. Lehman, J. Electrochemical Soc., **112**, 1013 (1965).

[11] Y.Kanzawa, S.Hayashi, K.Yamamoto, J.Phys.Condens. Matter **8**, 4823 (1996).

[12] P.G.Pai, S.S.Chao, Y.Takagi, G.Lucovsky, J .Vac.Sci.Technol. A. **4**, 689 (1986).

[13] M. Nakamura, Y. Mochizuki, K. Usami, Y. Itoh, T. Nozaki, Solid State Commun. **50**, 1079 (1984).

[14] A. Borgesi, B. Pivac, A. Sassella, A. Stella,. J.Appl. Phys. **77**, 4169 (1995).

[15] F. Giustino, A. Pasquarello, Phys. Rev. Lett. **95**, 187402 (2005).

[16] K. T. Queeney, M. K. Weldon, J. P. Chang, Y. J. Chabal, A. B. Gurevich, J. Sapjeta, R. L. Opila,. J.Appl. Phys. **87**, 1322 (2000).

[17] W.A.Pliskin, D.R.Kerr, and R.M.Perry in Physics of Thin Films, Vol.IV, ed. by G.Hass and R.B.Thun, Academic Press, New York and London 1967, article 5,

[18] Wei Cheng, Sh.-F. Ren., Phys.Rev.B **65** 205305 (2002).

[19] V.Paillard, P. Puech, M.A.Laguna, R.Carles, B.Kohn, F.Huisken, J. Appl. Phys. **86**, 1921 (1999).

*Corresponding author: ygoldst@vms.huji.ac.il